

Lawrence Berkeley National Laboratory

Recent Work

Title

FULL-SCALE MAGNETIC MEASUREMENTS ON THE BERKELEY 88-INCH CYCLOTRON

Permalink

<https://escholarship.org/uc/item/5ww9g2t5>

Author

Dorst, Joseph H.

Publication Date

1962-04-27

University of California
Ernest O. Lawrence
Radiation Laboratory

TWO-WEEK LOAN COPY

*This is a Library Circulating Copy
which may be borrowed for two weeks.
For a personal retention copy, call
Tech. Info. Division, Ext. 5545*

Berkeley, California

DISCLAIMER

This document was prepared as an account of work sponsored by the United States Government. While this document is believed to contain correct information, neither the United States Government nor any agency thereof, nor the Regents of the University of California, nor any of their employees, makes any warranty, express or implied, or assumes any legal responsibility for the accuracy, completeness, or usefulness of any information, apparatus, product, or process disclosed, or represents that its use would not infringe privately owned rights. Reference herein to any specific commercial product, process, or service by its trade name, trademark, manufacturer, or otherwise, does not necessarily constitute or imply its endorsement, recommendation, or favoring by the United States Government or any agency thereof, or the Regents of the University of California. The views and opinions of authors expressed herein do not necessarily state or reflect those of the United States Government or any agency thereof or the Regents of the University of California.

Journal and for UCLA Conf.

UNIVERSITY OF CALIFORNIA

Lawrence Radiation Laboratory
Berkeley, California

Contract No. W-7405-eng-48

FULL-SCALE MAGNETIC MEASUREMENTS ON
THE BERKELEY 88-INCH CYCLOTRON

Joseph H. Dorst

April 27, 1962

FULL-SCALE MAGNETIC MEASUREMENTS ON
THE BERKELEY 88-INCH CYCLOTRON

Joseph H. Dorst

Lawrence Radiation Laboratory
University of California
Berkeley, California

April 27, 1962

ABSTRACT

The measurements of midplane flux density as a function of position and current are described within the framework of a general plan for obtaining useful magnetic fields. Data were taken point-by-point in a radial direction on a grid of 1 in. by 3 deg. The separate effects of currents in the main coil and in the 17 circular trim coils were measured. The Theoretical Group calculated recommended currents and the predicted fields. The predicted fields for combinations of currents were verified by magnetic measurements at six probable operating levels. The harmonic content of the combined fields and the use of coils in the valleys for fine control of harmonics is described.

The operation of the flux density measuring system and the positioning systems is described. The flux density measuring system attained a resolution of $\frac{1}{2}$ G with a temperature-regulated Hall probe. The radial positioning was better than ± 0.005 in. using a tensioned metal tape. The azimuthal accuracy was better than 0.01 deg--by using precisely located pins on a fixed disk. Problems of current control and hysteresis are discussed.

Problems of data handling, and the use of a computer to find and correct errors are discussed. Final results are evaluated by comparison of predicted and measured fields.

FULL-SCALE MAGNETIC MEASUREMENTS ON
THE BERKELEY 88-INCH CYCLOTRON

Joseph H. Dorst

Lawrence Radiation Laboratory
University of California
Berkeley, California

April 27, 1962

1. Introduction

From January through August 1961, the magnet test group at our laboratory was responsible for making detailed measurements of the magnetic field of the 88-inch cyclotron. During the six weeks of the first phase (Phase I) of measuring, we determined the general suitability of the magnet, tried out and developed our tools, trained our personnel, and learned how to handle some of our problems. After another 11 weeks of preparation the magnet was turned over to us for Phase II of the measurements. We used 14 people for 11 weeks, with double-shift crews on the magnet and on the IBM data processing. We recorded approximately 400 000 separate readings. Now, after eight months, we have almost finished final processing of the measured data.

2. The Plan

The general purpose of the magnetic measurements was to obtain useful magnetic fields. Three ingredients which must be controlled in a useful magnet are: isochronism, focusing, and oscillations. The degree of control judged necessary or desirable bears directly on the question of what to measure and how to measure it. Both magnet development through the model program and theoretical analysis of the attained fields had shown that the particular hill design was suitable, and that there was sufficient capacity in the trim coils to produce useful fields for

*

Work done under the auspices of the U. S. Atomic Energy Commission.

all desired particles through most of the energy range, although the maximum possible energies were unknown. An examination of measurement philosophies has been written by Kelly; (ref ¹).) We wanted to set the magnet close enough to a fully useful field to be within "easy knob-twiddling range," whatever that is, and we wanted a high-quality beam and rapid flexibility in operation.

2.1 CONTROL OF OSCILLATIONS

Phase I, before installation of trim coils, was primarily a check of the magnet and of our measuring gear. We removed iron near the center to reduce an 8 - G first harmonic at 6 in. radius. We added iron at the very edge of the east valley (Valley A in fig. 1) to smooth out the rate of change of first harmonic due to the cross-overs in the main-coil conductors on the west side. We worried about the cross-overs in the leads to the trim coil platter (fig. 2), and added a small amount of iron in the north valley to precompensate their estimated effects. (The optimizing of the center region is covered by Watson in another report ².)

In the second phase, with trim coils, we calibrated the valley (harmonic) coils (fig. 3), and tested that we could make the first harmonic < 1 G for several inches at the end of acceleration. (The proposed deflector system begins at 39 in., which is beyond the point where $\sqrt{r} = 2 \sqrt{z}$): Fine control of the first harmonic has been achieved. See ref. ³) for a description of the method.

2.2 CONTROL OF ISOCRONISM AND FOCUSING

The main effort of Phase II was in measuring the iron, the trim coils, and the combined fields. The basic steps in the program for control of isochronism and focusing were:

- a. Measure in fine detail the "iron" fields in one sector (fig. 1),
- b. Measure in lesser detail the separate effects of changes of currents in the main coils and in the 17 circular trim coils,
- c. Calculate a set of optimum currents using azimuthally averaged main-coil and trim-coil effects,

- d. Predict the magnetic field in full detail, and
- e. Measure in fine detail the actual total field at the specified current.
field

The complete cycle was done at five/levels. The final measurements in each cycle were for a full 360 deg; these were known as Grand Tests. Additional sets of iron fields (with currents only in the main coils) were measured at many intermediate field levels, without the complete cycle of calculating and testing recommended currents.

3. Results of the Grand Tests

How well we did is difficult to describe. Figures 4, 5, 6, and 7 show the basic profiles for four of the Grand Tests. The adjustments to the actual measured values were simple calculations, due to small differences between the specified currents and the actual currents. The validity of the deviation is unaffected. In each of these cases the solution is for deuterons, and one of the iron maps is the base. The maximum phase slip, for the highest field, is about plus and minus 30 deg. The iron shapes at high field show the incompleteness of our optimizing at the "exit" radius. That radius changed from 37 in. to 39 in. as a result of deflector studies. The average radial profile of the isochronous fields is not shown on these graphs.

The deviation from prediction is shown amplified in fig. 3. The agreement in the gradient changes inside 25 in. is especially pleasing, and shows that the fields can be accurately known in the starting region from knowledge of the currents. The discrepancy near the outside edge is a valid failure of superposition in the region where the nonlinear effects are greatest. Note that Test No. V is actually poorer than No. I, although at a lower field. The deviations are obviously related to the total field change and the total gradient change. Everywhere the total changes are large. For instance, the predicted change in Test V at 32 in. is only + 27 G. But this was obtained by adding + 1033 G and - 1056 G. The net failure is only about 17 G. Additional iterations with the measured combined field as a base will be much

closer. Test VI was such an iteration, but the process of weeding out errors is not complete, and a precise comparison has not yet been made.

The measured fields in Tests II and III were sufficiently close to the predicted that particles could have been accelerated with phase slips of less than plus and minus 15 deg, with only slight changes in the main-coil current or in the accelerating frequency.

4. Measuring Equipment

The early decision to take data in a radial direction came directly from the evaluation of the azimuthally averaged radial gradient as the parameter requiring highest precision of measurement. The selection of 3 deg as the standard azimuthal increment came from analysis of the model data, which showed that 40 points per 120 deg sector were required to determine the average radial gradient of the total field to the requested precision of 1 G/in. For any single map, the required resolution of the flux density sensor could have been larger than the precision required of the average, because of the expected random nature of errors of resolution, but there are other important factors. The effects of each trim coil were measured with an azimuthal interval of 12 deg, which is only 10 points per sector. The predicted fields are the iron fields plus the algebraic sum of 18 separate trimming effects. For the desired precision in the total, the errors of a single element must be kept as low as possible. And finally, there are many possible variables in the measurement of flux density, as well as real time variations in the magnetic field. That is: the positioning equipment is never perfectly reproducible, the yardsticks used in flux density measurements are always slightly flexible, and the magnetic fields themselves are never absolutely stable. We measured with an extra factor in resolution in order to identify any variables, and correct the sources where possible.

Thus our overall plan of measurement placed a high premium on short-term reproducibility (with maximum resolution), a lesser premium on long-term reproducibility, and the lowest requirement on absolute value. These relative importances were applied to the three elements of the measurements: flux density, position, and currents.

4.1 FLUX DENSITY MEASUREMENT SYSTEM

- A. The system began with a stable current (about 99 mA) from a high-precision source.
- B. The current passed through a Hall plate.
- C. The Hall plate was held at a constant temperature by a separate subsystem.
- D. The Hall voltage was amplified by a fixed-gain ($\times 20$) D.C. amplifier.
- E. The output voltage was read by a digital voltmeter.
- F. The readings were recorded on punched cards.

Two elements of the system, the precision current sources and the temperature regulator, were powered through an A.C. line regulator (Sorensen Model 1000).

A. Current Sources - North Hills Electric Model CS-11). The current sources performed satisfactorily with some short-term noise of a few parts in 10^5 . No long term drift was detected. Our original intention was to use both sources in parallel to deliver about 200 mA. Unfortunately the thermal time constants of our original probe holder and oven were too long (and the performance of our original oven was terrible). As a result we thought that at 200 mA the variation of power in the probe with varying magnetic field was too high. In addition the current sources required occasional servicing, so we soon decided to use a single current source. The internal reference voltages of both sources were deliberately reduced to less than 10 V to permit frequent monitoring by direct reading into the voltmeter.

B. Hall Plates. These were Siemens FC-34. The dimensions of the sensitive elements are about 0.23 by 0.60 in. On the basis of uniform response from their area, the

maximum error in the measurement of the average gradient due to high third radial derivatives in the measured field was calculated to be about 1.4 G/in. at a radius of 39 in. Two plates were used in our series of measurements, Serial Nos. 702 and 634. The failure of No. 702 and the aging of No. 634 are discussed in a separate report by deForest⁴). All Phase II data was gathered with No. 634 in our best oven. The average sensitivity of this probe, at about 99 mA, was 22 uV/G.

C. Temperature Regulating System. The controller and oven assembly that were finally used worked extremely well. The first combination was completely unsatisfactory, primarily due to the very poor performance of a Robertshaw Fulton crystal oven. For all of Phase I, one model of the final brand of controller was used with some parts of the original oven, and this combination gave a lot of useful data. However, variations in Hall voltage, due to temperature swings, were several gauss and severely limited the measurements. Accurate determination of the first harmonic was very difficult, and the poor temperature control masked all other variables. (A rather large mistake was made, all too easily, when the Hall probe mounting cylinder was installed upside down. This resulted in all Phase I data being taken at 5/8 in. above the median plane).

Between the two periods of measurement, a resettable temperature controller and a new copper-sandwich Hall plate holder were tested. The last modification was to enclose the entire probe and heater assembly in an insulated brass box.

(1) Controller unit: this was a Hallikainen Instruments Thermotrol Model 1053A, which turned a thyatron on and off with a cycle time of about 1 sec. We used the output to drive a relay in a low-voltage 60-cycle heater circuit. The sensor was about 60Ω of platinum wire, wound noninductively and located on the midplane of the oven assembly. The inert resistor of the resistance bridge was also located in the oven. The adjustable arms of the bridge were primarily fixed resistors with a helipot only for the fine control. For our particular application, we rearranged

these resistors to make the two remote arms of the bridge have almost equal resistance (within 2%) when the probe was at the desired temperature of about 40°C. The actual set-point temperature was almost completely insensitive to heater voltage; that is, the unit would operate at the same temperature with a 10% or a 90% duty cycle. The monitoring of temperature was accomplished by measuring the voltage drop across the Hall current terminals at the Hall plate, and 18 "counts" was about 0.10°C. A simple test of the functioning of the system was available: We observed the settling time after making a step change of about 30% in the heater voltage. The "temperature" would swing off by 10 to 25 counts, and return to within one count within 20 sec.

In the usual operation, with only the input power variation with changes in magnetic field as a perturbing influence, the temperature was stable to plus and minus 0.01°C. The actual temperature of the semiconductor heart of the Hall plate did, of course, vary with the magnetic field, but it was only about 0.4 deg above the temperature of the sensor when in a 20 KG field. The time constant of this small part of the system was too short to measure accurately and did not affect our readings or our calibration. That is, we could not complete a measurement quickly enough to detect a transient state. With an operating range of $\pm 0.01^\circ\text{C}$ and a maximum measured temperature coefficient of Hall voltage of $-0.05\%/^\circ\text{C}$, the temperature regulation error was less than 1×10^{-5} , which is less than the resolution of the digital voltmeter.

(2) Hall probe and oven assembly: This is shown in fig. 9, 10, and 11. The probe block was made of copper. The shape of the copper block was designed so that the internal heat flow, of both the Hall plate and the sensor, was away from the midplane towards the flat sides. On the flat sides, the heater cards provide the necessary power to keep the block above ambient temperature and the heat flow is towards the flat sides of the brass box. The two heaters were bifilar windings of ordinary

fine magnet wire wound on cards. The terminal board for all leads was held at an almost constant temperature by locating it between the end fins of the block. The inert resistor was also in this space. The Hall plate and the temperature sensor were side by side in the midplane of the block. The insulation of Styrofoam reduced the required heater power to a relatively low level, and the brass box reduced any thermal gradients in the external environment. Additional construction details are in another report ⁴).

Overall checks of the sensitivity to ambient temperature were made from 15°C to 35°C. Although the heater current changed from 550 mA to less than 100 mA, the voltage drop across the current side of the Hall plate changed less than 2 counts, or about 0.01°C. The complete assembly could be placed with one flat side against a cold slab of metal with no noticeable effect on the set-point temperature. The normal level of power to the heaters was about 1 W, whereas the internal power to the probe and sensor was from 0.10 to 0.15 W.

D. Fixed - Gain Amplifier. Amplification was 20:1 (Ultronix matched resistors and Kintel Model 111A amplifier). The gain stability was primarily a function of the stability of two resistors. The first set of 20:1 was assembled in haste (when we changed the Hall current) and were 100 and 5K . With these low values the resistance of the voltage leads was a significant factor. Because of lead failures we had made changes to these leads before and during the measurements of Phase I. For Phase II we used a matched set of 1 M and 50K , and we calibrated and measured with the same leads. The amplifier could be replaced at any time without affecting the calibration. Output noise was never a problem during operation of the system.

E. Digital Voltmeter. This was a Non-Linear System Model V-35. For our use, the automatic ranging was disconnected and we read on the 10-V scale with an input

impedance of 1000 M . The maximum reading was plus or minus 9.9999 V. The least count was 100 uV. This voltmeter was both our pride and joy, and our despair. It was highly linear, to better than 5 parts per 100 000; highly stable, to better than 1 part in 20 000; and it was relatively insensitive to noise. Although not a fast DVM, it never required more than 2.3 sec to balance, and usually much less. But, it made mistakes. It did not come to balance on a wrong number very often, but when it did, that number went straight into the IBM cards. In hindsight, the condition of recording bad readings is entirely correctible, although our efforts during the testing were devoted to eliminating the incorrect reading of data, a process which was gradually more or less successful. (The very infrequent wrong decisions at some steps in the logic were due to wear in the transfer switch and the decade switches).

The recording of bad readings in our output data, increased our data processing costs by at least a factor of two, and the toleration of this error was the worst mistake we made. (A second "intolerable" error, which we had to accept, was the mispositioning of the azimuthal latch).

F. Data Recording. Output voltage readings were recorded on punched cards with an IBM Type 517 Summary Punch.

4.2 THE POSITIONING SYSTEM

The radial boom and the fixed mounting plate are shown in the magnet in fig. 12. The duraluminum plate is supported on posts that are visible in this picture, because the trim coils were not yet installed. The plate is centered on a stubby post which defines the magnet center. On the upper surface, the fixed azimuthal positioning pins are barely visible. There are 240 stainless steel pins, very precisely located. These pins locate the boom azimuthally by means of a latch mechanism. The minimum increment is 1 1/2 deg. and the polar grid is defined to

about 0.005 deg.

The radial boom is shown out of the magnet in fig. 13. The structure is about 140 in. long. The boat, with its arms guiding the cables to the cable trays, is at the far end, at about +50 in. The probe assembly is mounted under the boat. The range of radial motion is from -30 to +67 in. The azimuthal potentiometer is near the center, and the radial potentiometer is on the near end of the shaft of the drive sprocket. The shelf for mounting the NMR probe was not yet installed on the side of the channel. The assembly weighs about 200 lb, and is supported on four wheels and at the center bearing. The center bearing is just barely visible. The azimuthal latch mechanism is underneath the far end of the boom.

The main feature of this apparatus is the tape transport system. The close-up view in fig. 14 shows the drive train. The motor is about as large as we could get into the space available. The Geneva mechanism, with the control cams, was an excellent device. Rotation of the driven shaft 90 deg required about 0.2 sec; the cycle time was about 0.7 sec. The gear pair, shown engaged, was for 1 in. radial increment. The drive sprocket, precision tape, and the troublesome fixed and floating idlers are shown. Also visible is an early model of our edge-guide rollers. The guiding units were completely modified for use in the reduced gap of 5 1/2 in. when the trim-coil platters were installed.

There was doubt during the measurements, as to whether we would be able to finish taking data before the supply of tapes ran out. We checked every day for radial registration at the magnet center. Towards the end of the program the condition of the tape was constantly checked and small adjustments made. But the reproducibility was literally superb: 1 in. was 1 in. to better than 0.001 in. Over 6 - and 8 - hour stretches during our Grand Tests, the reproducibility at larger radius was checked with repeat runs, and we never had greater than 2-mil variation.

The backlash, or difference in position with direction of motion, was a function of radius, due to change in tension of the tape. It was about 5 mils at +50 in., but we always measured in the forward direction. The tape tension was about 60 lb.

The attainable azimuthal precision was very high, but setting and latching was a manual operation. Failure to properly position the azimuthal latch introduced errors in the measurement of flux density that were proportional to the azimuthal gradients. Radial runs that had large errors, on the order of 0.4 deg, were discovered relatively quickly, and about one-third were rerun. Most of those runs were tediously corrected by hand methods that were later refined into correction programs. Small angular position errors, less than 0.05 deg, usually were not readily detectable in the secondary processing, and a large number of them, perhaps 1% of all our runs, are gradually being eliminated from our data.

The operation of the radial mechanism and flux density measuring equipment was controlled at the double rack shown in fig. 15. The radial positioning was automatic, with several choices of start and return radii. A typical set of 68 points was measured while moving radially outwards; the probe was returned to the start point in a total elapsed time of 2.9 sec per point. The IBM punch determined the minimum time in flat fields, and the digital voltmeter plus the punch time set the maximum time in high-gradient fields.

4.3 CURRENT CONTROL AND HYSTERESIS

The setting of currents was the ultimate limiting factor in our measurements. The main-coil current was controlled with a voltage divider on the regulator reference voltage. Variations of the reference voltage supply during early measurements was one of the small factors that we found necessary to correct. Hysteresis was detectable at all field levels, but it was most severe below 12 kG. We were

not able to detect any changes in shape due to hysteresis, but the level of the field at 8 kG could be different by 60 or 70 G, depending on current history. To reduce the effect of hysteresis, the individual trim coils were measured at both polarities, and the trim-coil currents were set before the main field was brought back up to its final value. The setting of trim coil currents was a tedious task. Figure 16 shows two of the most important ingredients of our measurements: the humans at the endless task of setting and checking the currents during the measurements. The calibration of the current shunts in the power supplies was most important because many combinations of supply and coils are necessary for our optimum solutions.

4.4 DATA VALIDATION

The routine data processing was all done on an IBM 650. The processing section of the magnet test group was responsible for delivering valid data to the theoretical group. This difficult job was made almost impossible by the malfunctions of the voltmeter.

Since the conclusion of the measurements, computer programs have been developed by P. G. Watson and A. Albrecht to challenge our data and to correct the errors. Figure 17 is a display of part of an iron field map at 943 A. This is 30 deg data to 67 in. in Sector No. 1. For each point, a value is calculated by mesh interpolation from the adjacent 34 values. Figure 18 is a display of apparent errors, the differences between the calculated and measured values. Two values (-15516 and -2043) are wrong in this set of 680. The lower point indicates overlapping errors, since there is also a bad point at 90 deg. (as represented by the empty box). The upper point is alone and the reflections due to its error are outlined in a larger box. Note the symmetry of the numbers. The numbers outside the boxes show the random variation of our data, in tenths of gauss. The only values greater than 1 G are in a diagonal

strip just below center at the right. In this region, at the nose of a hill near the edge of the magnet, the interpolation scheme is not good enough to identify errors of < 2 G.

In fig. 19, the same error map is shown after partial corrections. The upper of the two bad values has been changed by 1551.4 G; the residuals within the large box are trivial. For the lower bad value the correction is incomplete. The computer must alternate between this point and the incorrect point at the neighboring azimuth; the process has not been finished. Each cycle of scanning 5500 values for the highest apparent error, correcting a single value, and recalculating the 35 values of the error matrix takes less than 4 sec on the IBM 709.

5. Conclusions

The most important conclusion is that we have an excellent magnet. The three-lobe symmetry is so strong that all fine structure in the magnetic field can be identified as to its source. The first-harmonic content of the fields at all radii is small and smooth, with or without the trim coils.

Secondly, toleration of the recording of bad data and irregular positioning is very costly: in time, money, and human effort. We did foresee most of the routine problems of handling bulk data, but the sheer quantity was not the problem. Whereas we recognized the necessity for taking and displaying data in a fashion that permitted detection of errors, but we woefully underestimated the time required for detection and for hand correction of poor data.

Finally, after our efforts to produce a highly stable flux density measuring system, it was a disappointment to uncover the apparent aging of Hall plates. Since there is also some limit to the possible speed with which we can take data with such a device, our enthusiasm for further development of Hall plates is rather low at this time.

Acknowledgments

Many people worked long and difficult hours to accomplish our mission and every man who participated deserves thanks. I am especially grateful to H. Thibeau, who supervised calibration of the current shunts in the power supplies, and daily calibration checks of the flux density system; to C. Markee, who supervised the processing section of the magnet test group; to T. Taylor for the mechanical design of the positioning equipment; and to S. Smiriga for the design and maintenance of the electronic equipment. Particular thanks are due to P. G. Watson for his supervision of the measurements, to C. G. Dols for his wise and patient counsel, and to E. L. Kelly for his excellent direction of the cyclotron project.

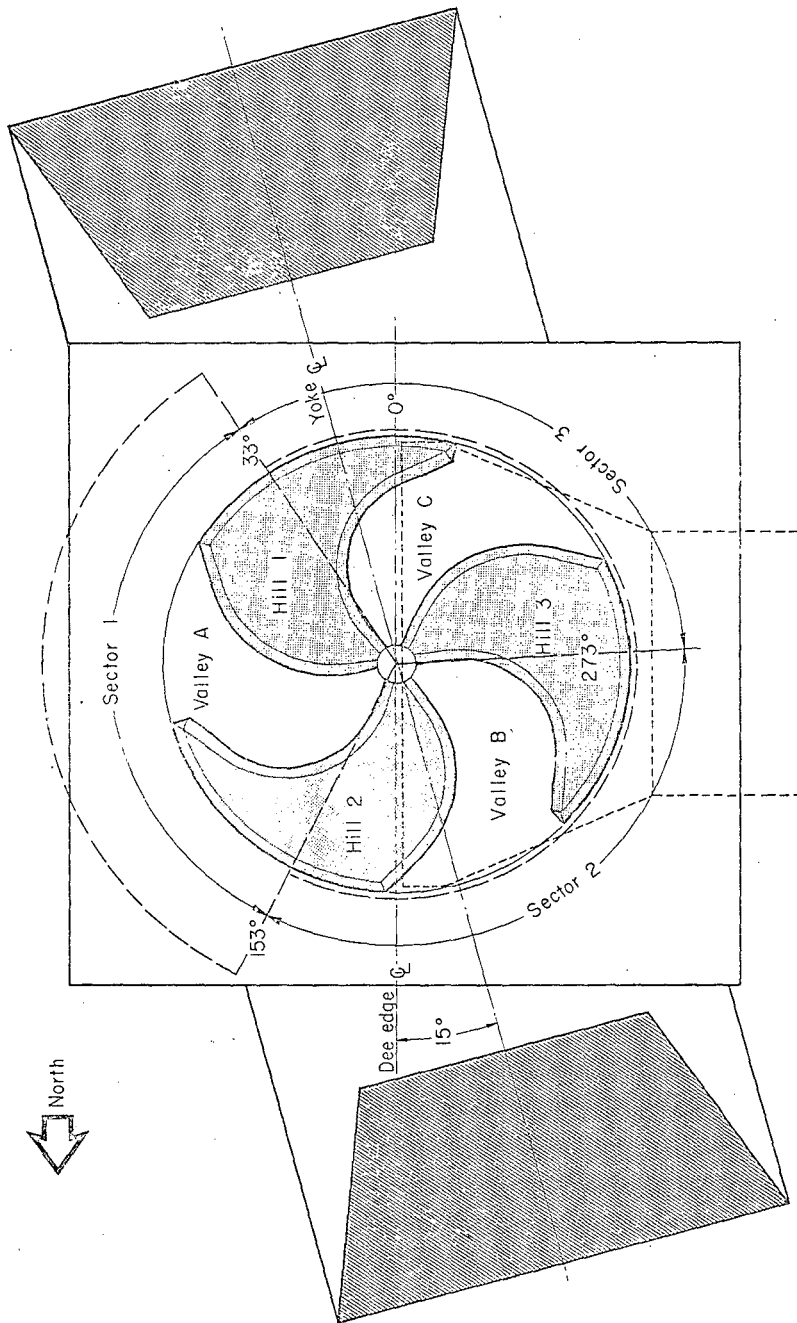
REFERENCES

- 1) E. L. Kelly, 88-Inch Cyclotron: Summary of Magnet-Measuring Discussions, Lawrence Radiation Laboratory Report UCID-1208, Aug. 1960 (unpublished).
- 2) P. G. Watson, Development of the Magnetic Cone for the Center of the Berkeley 88-Inch Cyclotron, Lawrence Radiation Laboratory Report UCRL-10072, May 1962, Nucl. Instr. and Meth. (to be published).
- 3) C. G. Dols, 88-Inch Cyclotron Magnet: Control of Azimuthal Position of Valley Coil Harmonics, Lawrence Radiation Laboratory Report UCID-1363, April 1960 (unpublished).
- 4) R. de Forest, A Hall Probe Assembly for the Berkeley 88-Inch Cyclotron, Lawrence Radiation Laboratory Report UCRL-10085, March 1962, Nucl. Instr. and Meth. (to be published).

FIGURE CAPTIONS


- Fig. 1. Plan view of magnet. (Pole diameter = 88 in.; Sector 1 measured to R = 67 in.; Sectors 2 and 3 measured to R = 45 in.).
- Fig. 2. Trim-coil leads and cross-overs.
- Fig. 3. Valley coils. (Pole side of upper coils, in position for brazing).
- Fig. 4. Average radial profile: Grand Test I. (Iron curve: main coil at 2090 A; Predicted and Measured curves: main coil at 2371 A, plus trim coils).
- Fig. 5. Average radial profile: Grand Test II. (Iron curve: main coil at 765 A; Predicted and Measured curves: main coil at 805; plus trim coils).
- Fig. 6. Average radial profile: Grand Test IV (Iron curve: main coil at 1470 A; Predicted and Measured curves: main coil at 1622 A, plus trim coils).
- Fig. 7. Average radial profile: Grand Test V (Iron curve: main coil at 1840 A; Predicted and Measured curves: main coil at 2106 A, plus trim coils).
- Fig. 8. Deviation from predicted field.
- Fig. 9. Hall probe and oven: complete assembly.
- Fig. 10. Hall probe and oven: partially open.
- Fig. 11. Hall probe and oven: midplane exposed.
- Fig. 12. The 88-inch cyclotron magnet: magnet-measuring equipment installed.
- Fig. 13. Radial boom.
- Fig. 14. Radial boom (close up of motor end).
- Fig. 15. Magnet testing console.
- Fig. 16. Operators setting and checking currents.
- Fig. 17. Computer output display of measured flux density (in gauss).
- Fig. 18. Computer output field error display before correction (values are tenths of gauss).
- Fig. 19. Computer output field error display after partial correction (values are tenths of gauss).

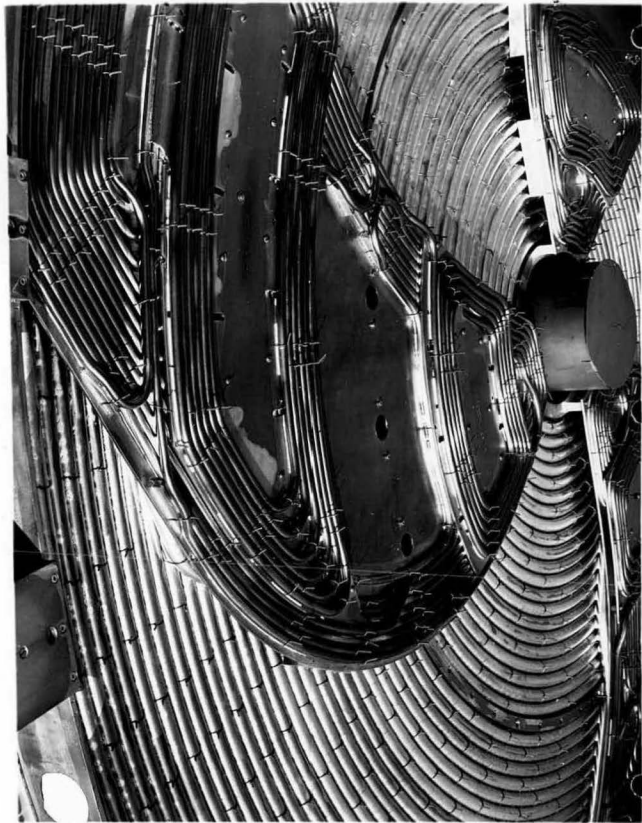
MUR-1016
UCRL-10074
Fig. 1



INFORMATION DIVISION
LAWRENCE RADIATION LABORATORY
UNIVERSITY OF CALIFORNIA
BERKELEY, CALIFORNIA

88" CYC. 159


PHOTOGRAPHED BY BERKELEY
 GRAPHIC ARTS
UNIVERSITY OF CALIFORNIA

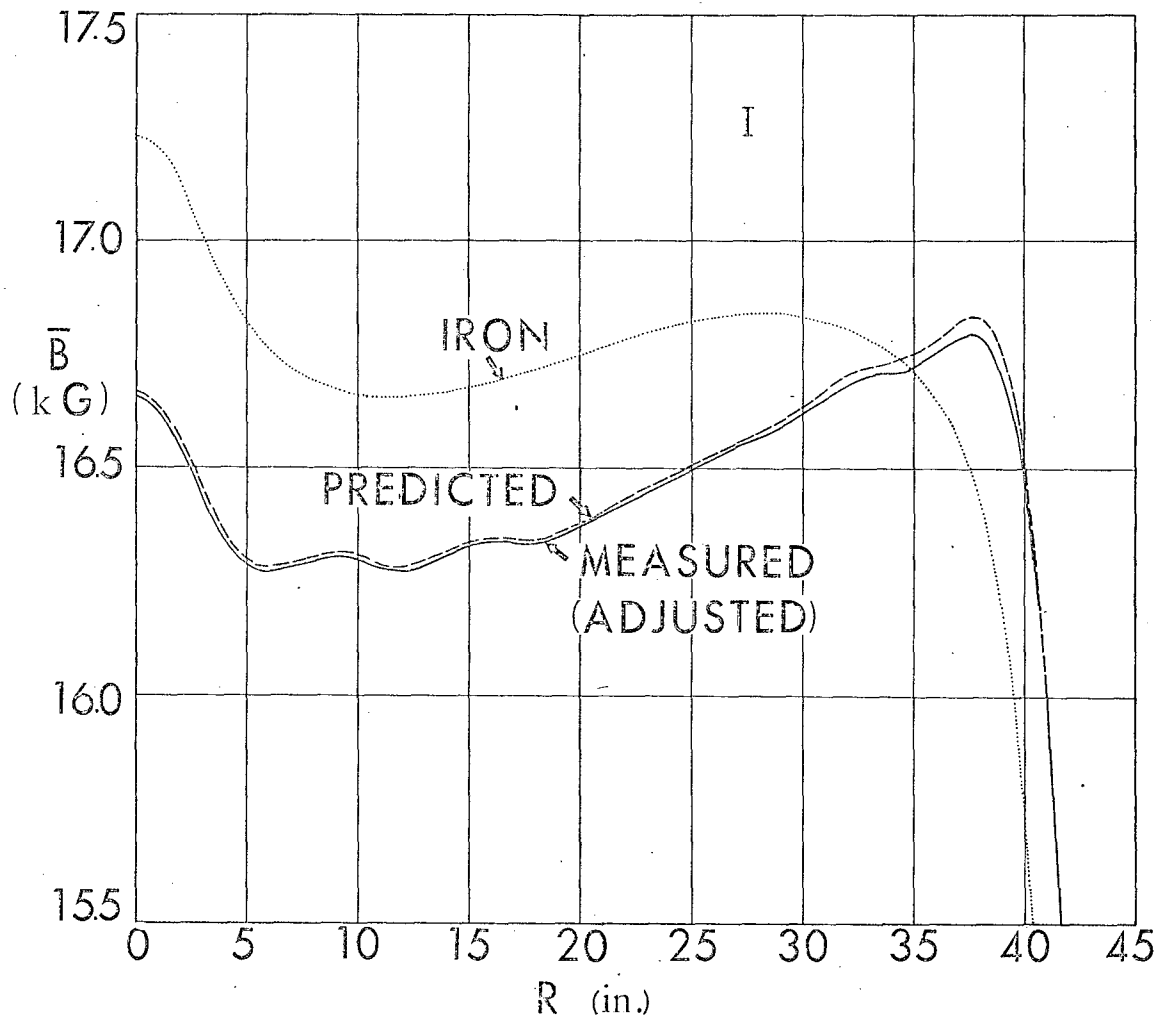


3

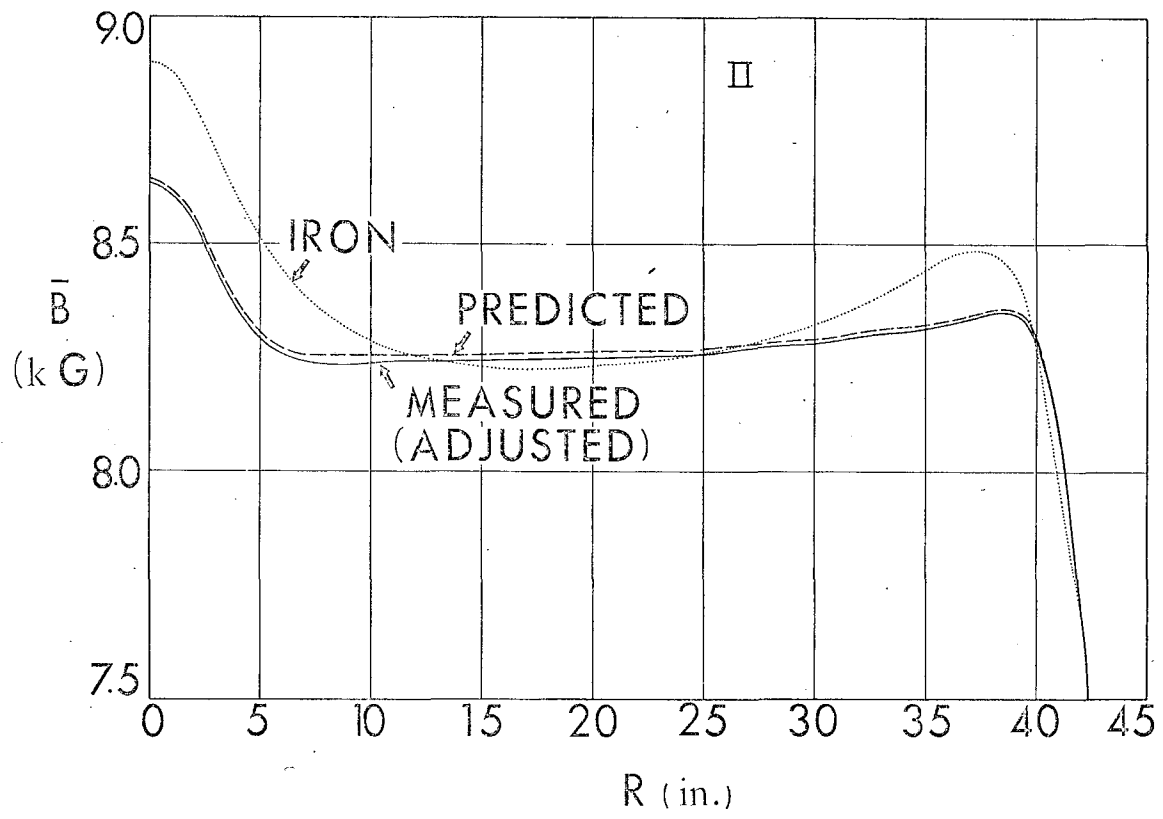
INFORMATION DIVISION
LAWRENCE RADIATION LABORATORY
UNIVERSITY OF CALIFORNIA
BERKELEY, CALIFORNIA

88th CYC - 494

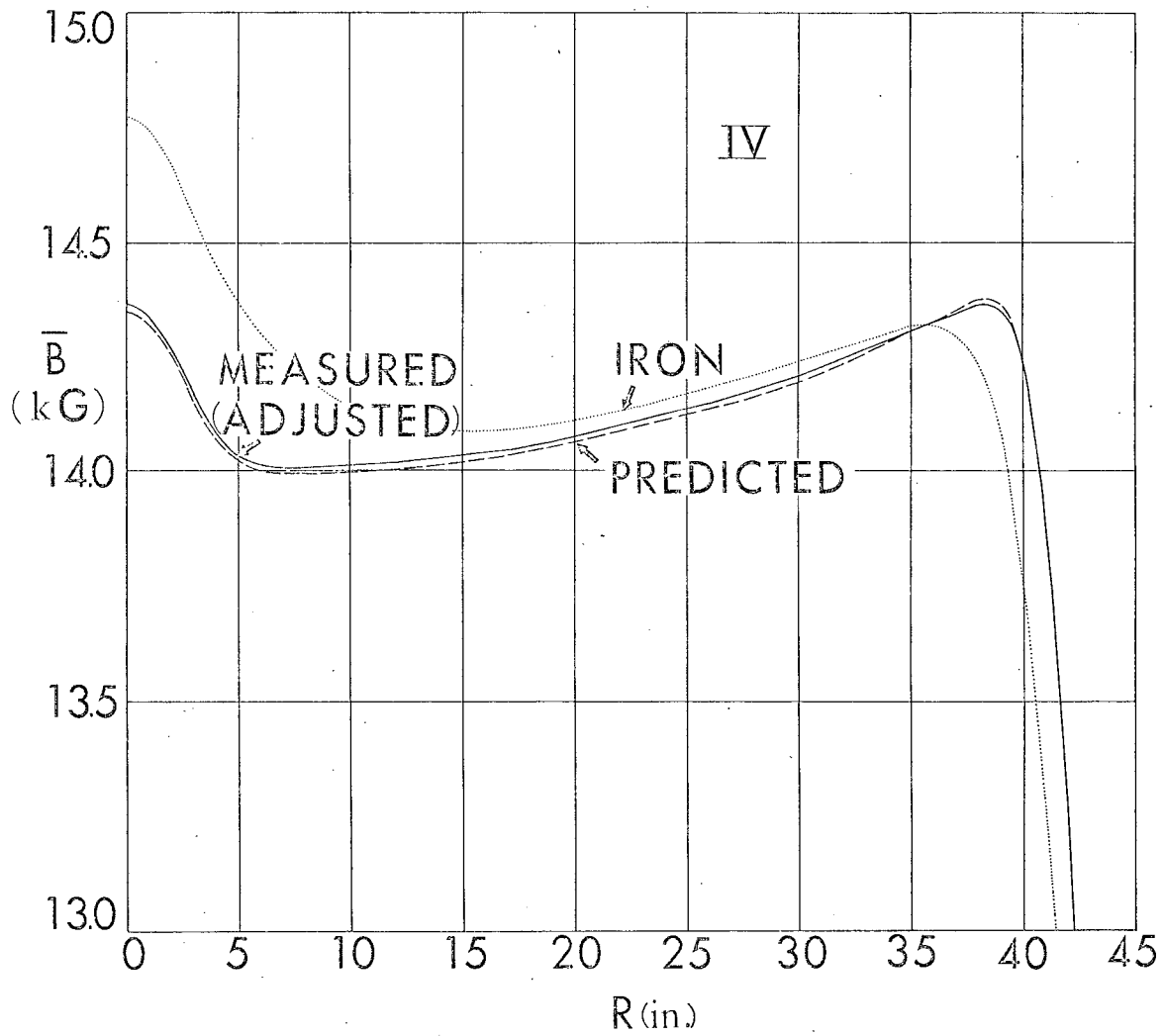
PHOTOGRAPHED BY BERKELEY
 GRAPHIC ARTS
UNIVERSITY OF CALIFORNIA



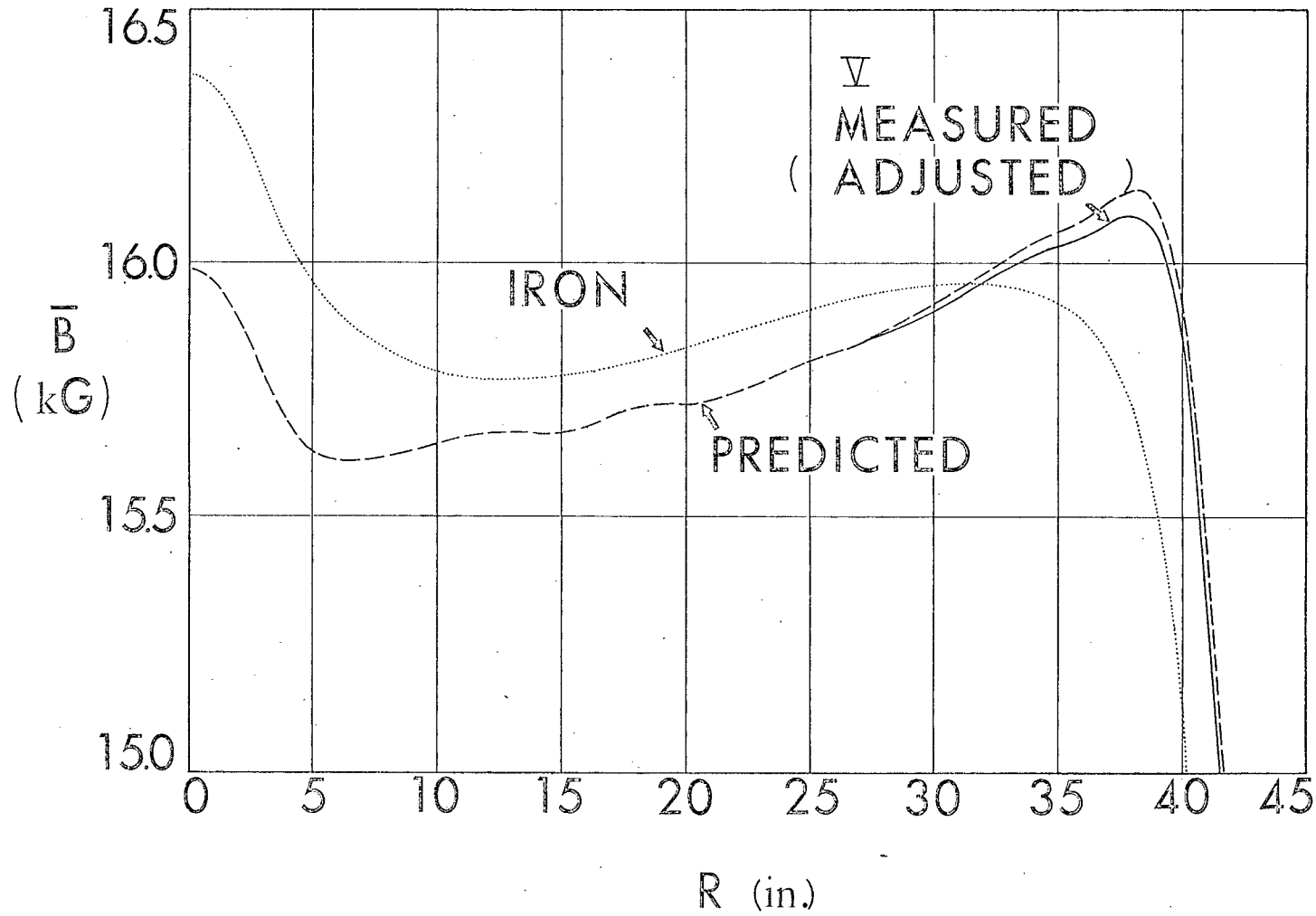
MUB-1059
UCRL-10074
Fig. 4



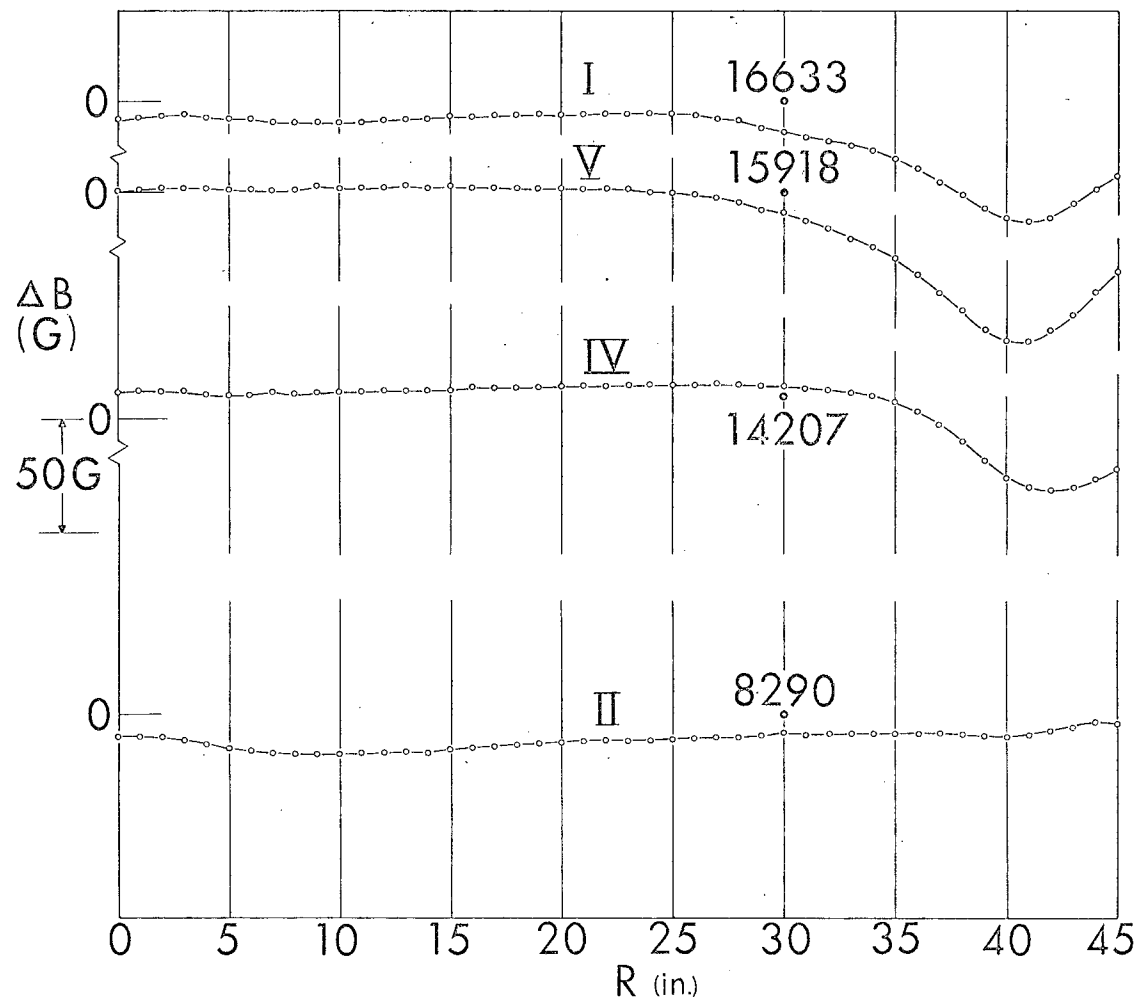
MUB-1060
 UCRL-10074
 Fig. 5



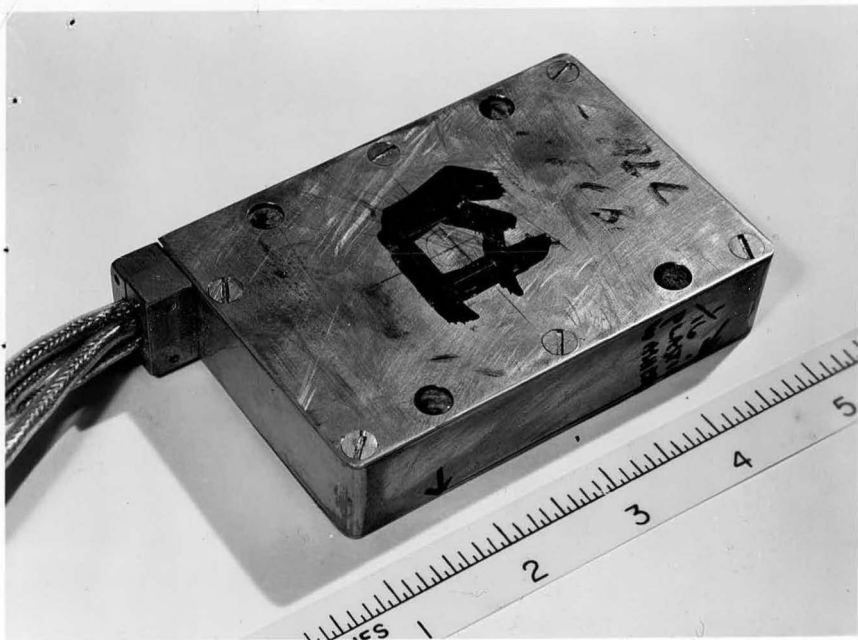
MUR-1061
UCRL-10074
Fig. 6



MIB-1062
 UCRL-10074
 Fig. 7




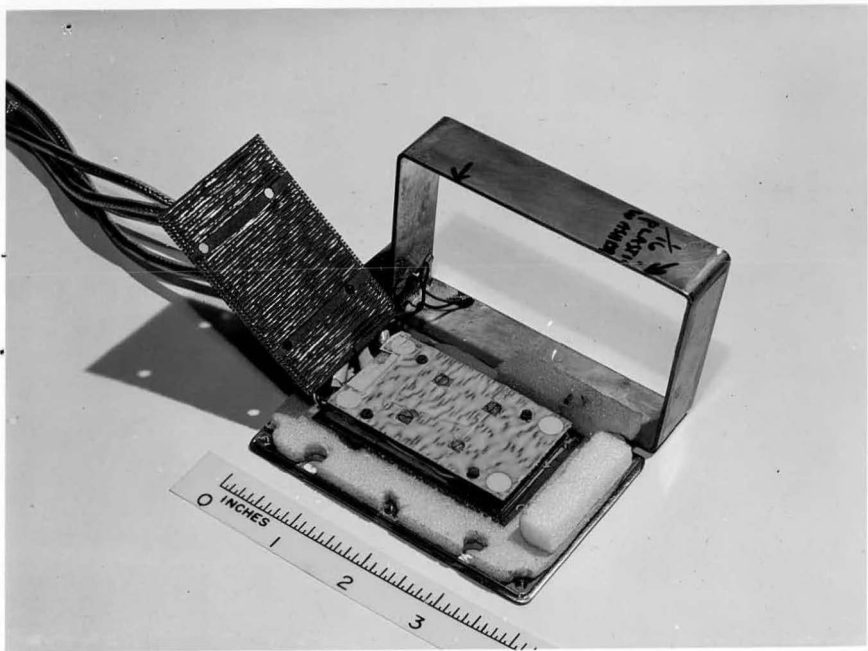
MRB 1063
 UCRL-10074
 Fig. 8



INFORMATION DIVISION
LAWRENCE RADIATION LABORATORY
UNIVERSITY OF CALIFORNIA
BERKELEY, CALIFORNIA

88"CYC-4771


PHOTOGRAPHED BY BERKELEY
 GRAPHIC ARTS
UNIVERSITY OF CALIFORNIA

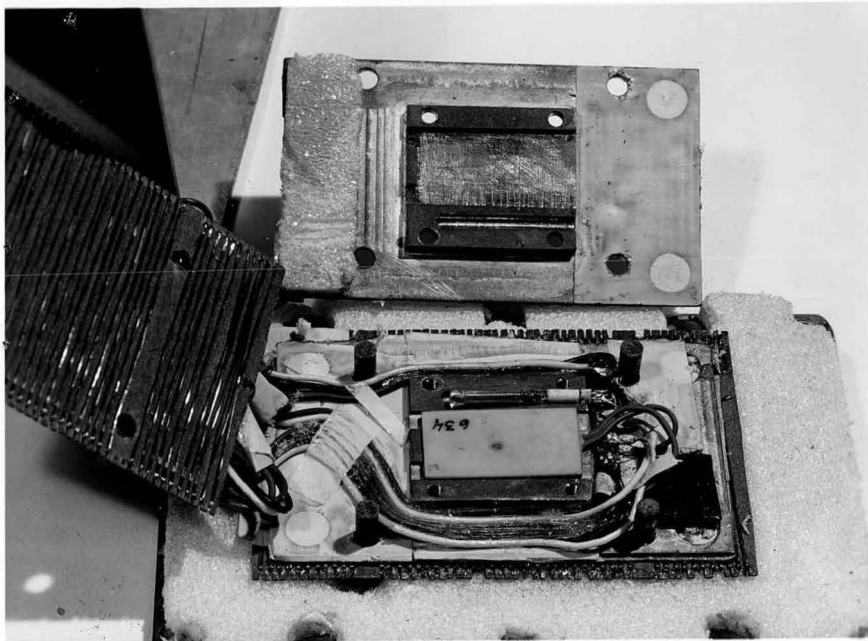


10

INFORMATION DIVISION
LAWRENCE RADIATION LABORATORY
UNIVERSITY OF CALIFORNIA
BERKELEY, CALIFORNIA

88th CYC - 478

PHOTOGRAPHED BY BERKELEY
 GRAPHIC ARTS
UNIVERSITY OF CALIFORNIA

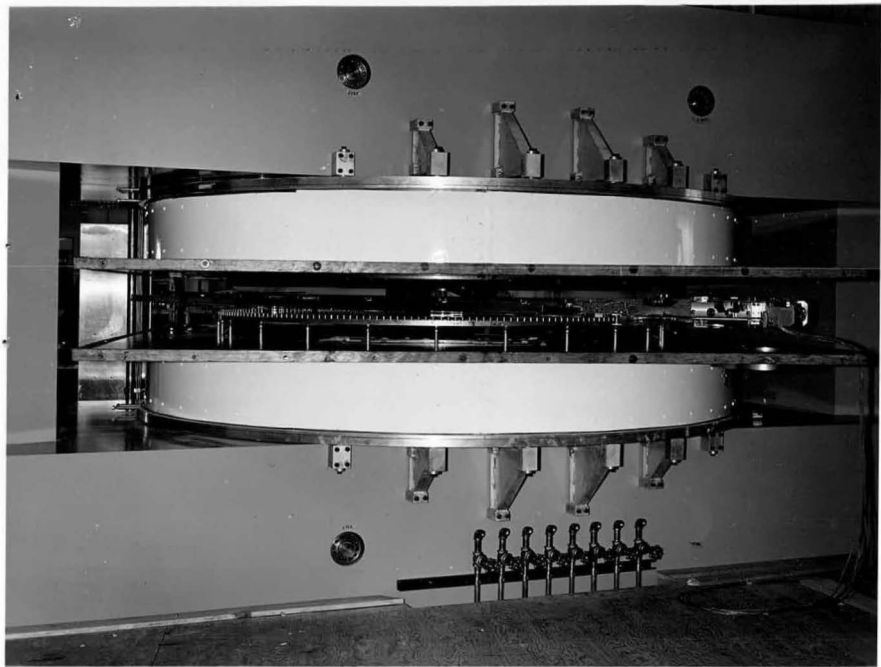


11

UNIVERSITY OF CALIFORNIA
GRAPHIC ARTS
PHOTOGRAPHED BY BERKELEY


INFORMATION DIVISION
LAWRENCE RADIATION LABORATORY
UNIVERSITY OF CALIFORNIA
BERKELEY, CALIFORNIA

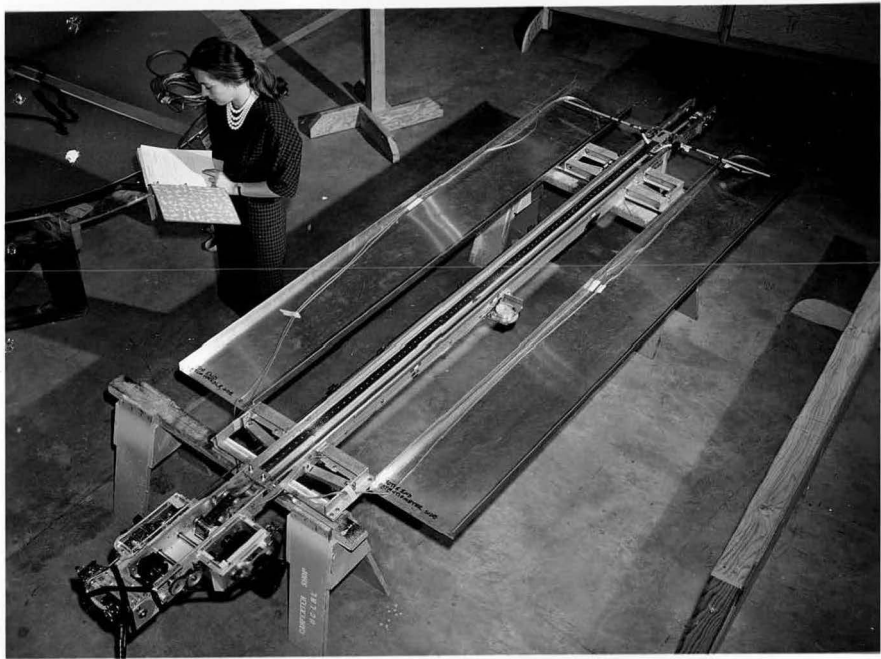
88"CYC. 479



INFORMATION DIVISION
LAWRENCE RADIATION LABORATORY
UNIVERSITY OF CALIFORNIA
BERKELEY, CALIFORNIA


88" CYC - 292

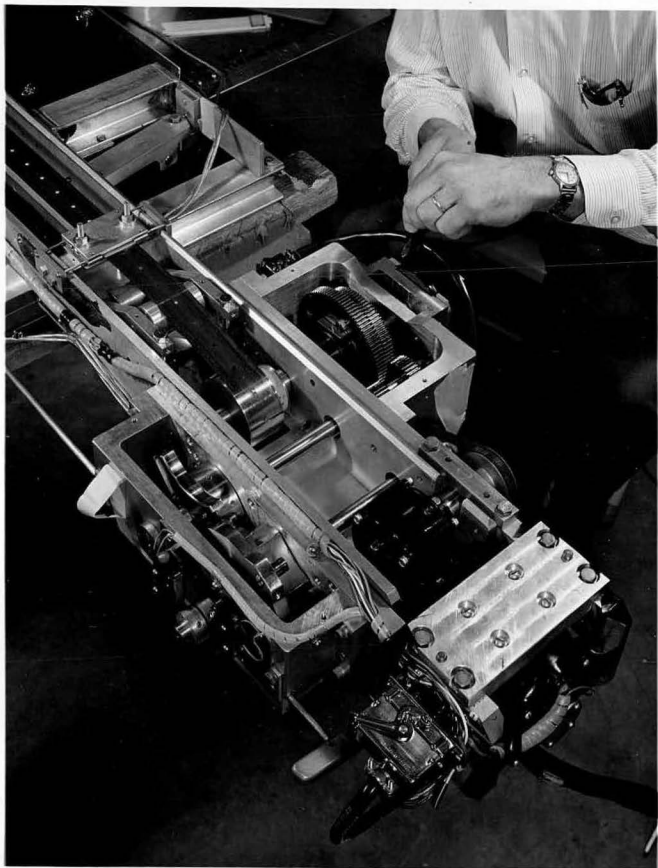
PHOTOGRAPHED BY BERKE
 GRAPHIC ART
UNIVERSITY OF CALIFOR



INFORMATION DIVISION
LAWRENCE RADIATION LABORATORY
UNIVERSITY OF CALIFORNIA
BERKELEY, CALIFORNIA

88" CYC. 299

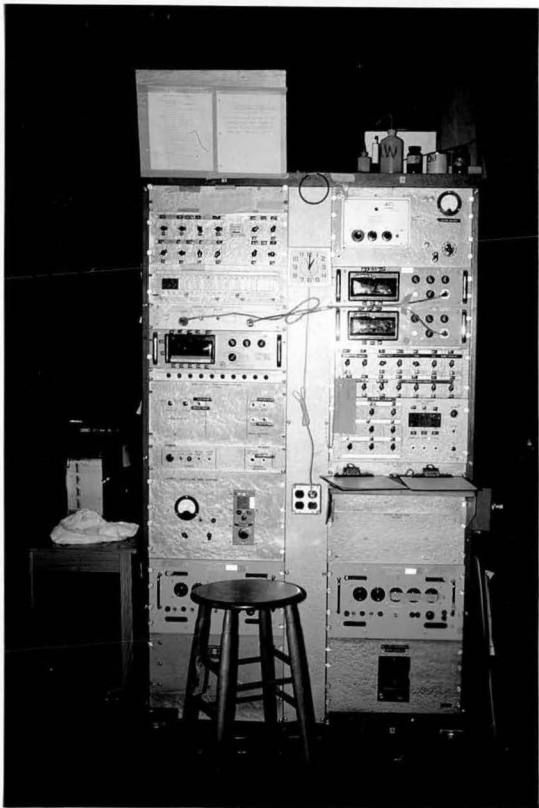
PHOTOGRAPHED BY BERKELEY
 GRAPHIC ARTS
UNIVERSITY OF CALIFORNIA



PHOTOGRAPHED BY BERKELEY
 GRAPHIC ARTS
UNIVERSITY OF CALIFORNIA

INFORMATION DIVISION
LAWRENCE RADIATION LABORATORY
UNIVERSITY OF CALIFORNIA
BERKELEY, CALIFORNIA

88th CYC. 296



PHOTOGRAPHED BY BERKELEY
LRL GRAPHIC ARTS
UNIVERSITY OF CALIFORNIA

INFORMATION DIVISION
LAWRENCE RADIATION LABORATORY
UNIVERSITY OF CALIFORNIA
BERKELEY, CALIFORNIA

88"CYC- 565]



MAY 21 1982

NOT FOR PUBLICATION WITHOUT PERMISSION

INFORMATION & LIBRARY
LAWRENCE RADIATION LABORATORY
UNIVERSITY OF CALIFORNIA
BERKELEY, CALIFORNIA

88" CYC - 569

PHOTOGRAPHED BY BERKELEY
 GRAPHIC ARTS
UNIVERSITY OF CALIFORNIA

BL MAP OF KUNS 2 TO 2065. MAGNET CURRENT 943 AMPS.

RADIUS / THETA	93	96	99	102	105	108	111	114	117	120
0.	10763.0	10763.0	10763.0	10763.0	10763.0	10763.0	10763.0	10763.0	10763.0	10763.0
1.0	10741.0	10740.1	10738.5	10737.1	10735.1	10734.0	10732.8	10732.1	10731.5	10731.5
2.0	10684.8	10674.6	10664.0	10653.8	10644.1	10634.9	10625.1	10619.1	10613.0	10608.2
3.0	10615.9	10591.9	10547.8	10514.1	10482.2	10452.2	10425.3	10402.0	10382.5	10367.8
4.0	10563.6	10489.1	10414.7	10342.1	10273.5	10209.5	10153.0	10103.8	10064.1	10033.3
5.0	10542.1	10414.4	10288.0	10164.8	10050.0	9944.8	9851.5	9771.7	9707.6	9658.4
6.0	10541.7	10357.0	10174.8	9999.3	9836.4	9688.9	9559.9	9451.1	9364.0	9298.3
7.0	10546.9	10308.8	10073.5	9849.4	9643.1	9458.9	9299.7	9167.8	9063.0	8985.4
8.0	10553.2	10266.3	9983.2	9715.8	9472.8	9258.8	9077.4	8929.2	8813.8	8729.3
9.0	10558.2	10225.8	9899.0	9593.3	9319.9	9083.3	8887.5	8730.7	8610.4	8524.4
10.0	10557.0	10181.6	9814.7	9475.6	9178.2	8927.1	8723.6	8564.6	8445.8	8362.1
11.0	10542.6	10125.8	9722.0	9356.0	9041.6	8783.5	8579.7	8424.3	8311.1	8234.0
12.0	10537.6	10051.7	9616.1	9230.0	8907.1	8649.7	8452.1	8305.8	8201.8	8132.9
13.0	10446.6	9953.2	9492.3	9094.8	8772.7	8523.7	8337.7	8204.9	8112.6	8053.6
14.0	10355.4	9829.7	9300.3	8952.4	8639.8	8405.7	8237.1	8119.5	8040.2	7991.6
15.0	10233.2	9683.7	9196.2	8806.1	8511.4	8298.0	8148.7	8048.3	7982.5	7943.6
16.0	10080.3	9511.6	9031.9	8661.3	8390.8	8201.8	8073.8	7989.7	7937.3	7907.1
17.0	9898.5	9325.5	8863.6	8521.0	8280.8	8117.9	8010.9	7942.9	7901.3	7880.0
18.0	9693.0	9130.5	8698.3	8390.7	8183.1	8046.7	7959.6	7905.7	7874.6	7859.8
19.0	9470.8	8934.1	8541.7	8273.6	8098.9	7987.4	7918.3	7877.2	7854.5	7845.9
20.0	9241.2	8745.3	8399.3	8172.1	8028.5	7939.8	7896.3	7855.9	7840.3	7836.6
21.0	9012.7	8568.6	8272.9	8085.8	7971.1	7902.0	7851.5	7840.1	7830.3	7831.0
22.0	8795.7	8410.6	8165.2	8015.1	7925.4	7872.8	7843.4	7828.7	7824.5	7829.6
23.0	8597.1	8274.3	8075.9	7958.3	7890.1	7851.4	7830.6	7821.7	7821.7	7831.0
24.0	8424.4	8160.5	7800.3	7914.4	7863.7	7835.7	7822.1	7818.3	7822.4	7836.8
25.0	8277.5	8068.5	7948.7	7880.8	7844.4	7825.2	7817.4	7818.3	7827.3	7847.3
26.0	8157.1	7976.1	7905.8	7856.6	7830.9	7819.2	7816.3	7821.5	7835.9	7864.2
27.0	8061.5	7940.6	7874.7	7839.7	7822.6	7816.6	7818.6	7829.4	7851.4	7890.2
28.0	7988.9	7899.8	7852.5	7828.1	7818.4	7817.6	7825.1	7842.6	7874.6	7929.2
29.0	7934.8	7870.6	7837.6	7822.1	7818.2	7822.9	7837.1	7854.4	7910.4	7987.9
30.0	7896.5	7851.5	7829.0	7820.4	7821.9	7833.1	7856.6	7897.6	7965.4	8075.1
31.0	7872.2	7841.1	7826.9	7823.9	7831.4	7851.0	7887.5	7949.4	8048.7	8205.1
32.0	7859.4	7838.8	7830.9	7833.2	7847.4	7878.6	7934.6	8027.7	8173.4	8395.3
33.0	7858.9	7845.7	7843.2	7850.4	7873.4	7920.8	8005.8	8145.6	8357.9	8668.6
34.0	7870.8	7863.4	7864.5	7877.8	7912.4	7983.0	8110.8	8318.7	8624.0	9045.4
35.0	7896.8	7893.5	7898.4	7917.9	7968.1	8072.1	8252.0	8566.0	8991.6	9534.1
36.0	7936.2	7935.8	7943.6	7971.5	8041.7	8192.4	8469.6	8898.7	9461.6	10104.7
37.0	7982.6	7984.2	7994.9	8031.7	8129.9	8345.5	8739.3	9317.9	10005.9	10683.6
38.0	8018.0	8021.5	8034.9	8082.1	8215.4	8518.4	9058.7	9788.1	10541.6	11154.4
39.0	8014.6	8019.2	8035.2	8093.2	8267.2	8579.2	9384.1	10226.2	10944.5	11414.5
40.0	7937.4	7942.7	7961.7	8029.1	8244.6	8771.6	9623.2	10492.2	11084.7	11397.9
41.0	7756.2	7761.3	7783.1	7857.6	8104.9	8718.7	9638.9	10429.1	10860.8	11051.4
42.0	7452.7	7458.0	7480.7	7558.2	7816.6	8445.6	9338.1	9941.4	10233.7	10347.7
43.0	7025.2	7030.8	7053.0	7128.0	7371.3	7930.6	8527.5	9085.5	9278.8	9350.1
44.0	6493.8	6499.2	6520.4	6588.7	6795.4	7232.7	7732.9	8043.2	8172.0	8219.9
45.0	5887.4	5892.4	5910.7	5970.0	6131.4	6441.4	6773.1	6976.3	7053.5	7097.4
46.0	5250.0	5254.8	5271.3	5319.0	5437.7	5644.5	5855.0	5988.2	6048.2	6073.4
47.0	4622.6	4627.0	4641.3	4678.8	4762.8	4896.2	5029.3	5115.6	5158.2	5177.4
48.0	4036.9	4041.1	4053.0	4081.6	4139.8	4226.0	4310.6	4367.8	4398.2	4412.5
49.0	3505.4	3509.0	3518.9	3540.7	3580.8	3636.5	3690.9	3729.8	3751.7	3763.2
50.0	3032.5	3035.4	3043.3	3060.1	3088.4	3124.9	3160.1	3187.1	3203.4	3212.3
51.0	2615.4	2617.9	2624.6	2637.5	2657.8	2682.1	2705.9	2724.6	2736.7	2744.0
52.0	2252.1	2254.4	2259.9	2269.8	2284.6	2301.3	2317.4	2330.7	2339.9	2345.9
53.0	1933.5	1935.8	1939.8	1947.8	1958.7	1970.4	1981.7	1991.5	1998.5	2002.8
54.0	1656.1	1658.1	1661.6	1667.6	1675.7	1684.2	1692.5	1699.5	1705.3	1708.6
55.0	1414.9	1416.9	1420.0	1424.5	1430.6	1438.6	1442.6	1448.4	1452.4	1454.9
56.0	1207.4	1208.9	1211.4	1215.4	1219.8	1224.3	1229.1	1233.1	1236.4	1238.4
57.0	1027.8	1029.8	1031.6	1034.6	1037.9	1041.7	1045.2	1048.5	1050.5	1052.3
58.0	874.6	876.1	878.1	880.1	882.7	885.9	888.4	891.0	892.7	893.5
59.0	744.0	745.5	747.0	748.8	750.6	753.1	755.3	757.3	758.6	759.1
60.0	633.5	635.0	636.2	637.8	639.3	641.0	643.3	644.6	645.6	645.8
61.0	540.1	541.1	542.4	543.4	544.7	545.5	547.9	549.2	549.7	550.0
62.0	461.2	462.2	463.2	463.9	465.0	465.5	467.7	468.5	469.0	469.2
63.0	394.3	395.0	396.3	397.0	398.1	399.1	399.8	400.8	400.8	400.6
64.0	338.2	339.5	340.0	340.5	341.3	342.3	343.0	343.8	343.8	343.5
65.0	290.8	291.8	292.3	293.1	293.6	294.3	295.1	295.3	295.3	295.1
66.0	250.7	251.4	252.2	252.7	253.2	253.9	254.4	254.7	254.7	254.4
67.0	216.6	217.3	217.8	218.3	219.1	219.4	219.9	220.1	219.9	219.9

UCRL-10074

Fig. 17

10X(B1 - B1 CALCULATED RADIALLY 5 AZI. BY 7 RAD. MESH) ON RUNS 0 TO 2065. MAGNET. CURRENT 943 AMPS.

RADIUS / THETA	93	96	99	102	105	108	111	114	117	120
0.	-3	-3	-3	-3	-3	-3	-3	-3	-3	-3
1.0	-2	2	0	-2	2	-2	3	-3	-3	2
2.0	-1	0	-2	2	-2	3	-3	1	2	-4
3.0	3	-2	3	-2	1	-3	1	1	-3	5
4.0	-1	2	-4	3	1	-2	2	-2	3	-3
5.0	-1	-3	3	-2	-1	3	-2	1	-1	0
6.0	4	-2	-3	1	1	-3	3	-2	1	-3
7.0	-5	3	-1	1	-1	2	-3	4	-3	2
8.0	3	-1	1	-1	-3	0	2	-4	5	-3
9.0	-1	1	-2	1	1	-2	0	4	-5	4
10.0	-2	-3	3	-2	-3	2	-1	-2	5	-4
11.0	134	-519	774	-515	129	0	-3	2	-3	2
12.0	-783	3137	-4654	3132	-775	-3	3	-2	2	3
13.0	1947	-7762	11637	-7757	1938	5	-6	4	-3	-3
14.0	-2594	10349	-15516	10343	-2585	-5	7	-5	1	3
15.0	1946	-7763	11639	-7760	1941	3	-7	7	-4	0
16.0	-780	3137	-4658	3137	-779	-1	5	-8	8	-4
17.0	132	-520	778	-520	132	-3	-4	8	-9	6
18.0	-2	2	-1	1	-2	1	2	-5	6	-4
19.0	2	-3	1	-1	2	-1	-1	3	-3	2
20.0	-1	2	-1	2	-2	0	2	-3	2	1
21.0	15	-67	102	-69	18	1	-4	4	-1	-2
22.0	-98	404	-511	409	-192	-3	4	-3	0	3
23.0	37	-962	1530	-1022	255	2	-2	1	2	-3
24.0	937	1040	-2343	1364	-342	-1	1	1	-3	4
25.0	-2926	-227	1535	-1026	258	-1	-3	-1	4	-5
26.0	4137	-649	-616	411	-104	1	1	1	-4	5
27.0	-3163	726	103	-67	17	0	-2	1	2	-3
28.0	1272	-318	1	-2	2	-1	3	-3	2	-1
29.0	-213	51	0	-1	1	-1	-3	5	-5	4
30.0	-4	3	-2	1	-1	-1	3	-4	4	-2
31.0	5	-4	3	-3	1	0	-2	3	-2	-1
32.0	-4	5	-4	3	-2	0	1	-2	1	1
33.0	4	-5	6	-4	1	0	-1	2	-2	1
34.0	-2	5	-7	5	-2	-1	2	-3	2	3
35.0	0	-3	7	-7	3	1	-4	4	2	2
36.0	-3	3	-5	6	-4	-2	3	0	4	-15
37.0	2	-2	3	-3	1	-1	0	8	-16	3
38.0	-3	1	0	-1	0	-1	9	-15	0	14
39.0	3	-1	-1	2	-2	8	-9	-6	14	-2
40.0	-2	2	-1	-3	6	0	-11	9	4	-7
41.0	0	-2	2	1	-3	-7	2	15	-12	-1
42.0	2	-3	-3	3	-5	-8	20	-10	-2	1
43.0	-2	3	-2	-1	-3	10	-5	-5	3	3
44.0	1	-5	6	-4	3	3	-6	2	2	-2
45.0	1	4	-8	5	2	-2	-1	-3	1	2
46.0	-2	-2	5	-3	-1	-3	0	3	-1	-4
47.0	2	-3	-1	1	1	-2	1	-1	-1	4
48.0	-2	1	-3	0	-2	2	0	-1	3	-4
49.0	1	-1	1	0	1	-2	1	1	-3	1
50.0	-1	1	-1	0	-1	3	-3	0	2	0
51.0	1	0	-3	0	1	-3	2	-3	-3	-3
52.0	-1	-2	3	-2	-3	1	-3	-1	0	-3
53.0	1	3	-3	2	0	0	-3	4	-2	1
54.0	-1	-2	1	0	-1	-1	5	-6	3	-3
55.0	-1	2	1	-2	1	2	-6	7	-4	-1
56.0	4	-4	1	1	-3	-2	5	-7	5	0
57.0	-6	6	-3	1	-1	1	-3	5	-5	2
58.0	4	-5	4	-3	1	-1	1	-3	4	-2
59.0	-1	1	-1	2	-2	3	-3	3	-2	1
60.0	-1	2	-2	-3	3	-5	5	-4	2	0
61.0	1	-3	3	-1	-2	4	-6	5	-2	-2
62.0	-1	4	-3	1	-3	-2	4	-4	1	3
63.0	3	-5	3	-1	1	-3	-2	2	-3	-4
64.0	-3	4	-1	-3	-1	2	-1	0	-3	3
65.0	1	0	-2	2	1	-3	3	-2	0	-1
66.0	2	-3	3	-2	-1	3	-3	1	1	0
67.0	-3	-3	-3	-3	-3	-3	-3	-3	-3	-3

UCRL-10074
Fig. 18

SURVEY

47 1752

10X(B2 - B2 CALCULATED RADIALLY 5 AZI. BY 7 RAD. MESH) ON RUNS 0 TO 2065. MAGNET CURRENT 943 AMPS

RADIUS / THETA	93	96	99	102	105	108	111	114	117	120
0.	-0	-0	-0	-0	-0	-0	-0	-0	-0	-0
1.0	-2	2	0	-2	2	-2	3	-3	-0	2
2.0	-1	0	-2	2	-2	3	-3	1	-2	-4
3.0	3	-2	3	-2	1	-0	1	1	-3	5
4.0	-1	2	-4	3	1	-2	2	-2	3	-3
5.0	-1	-0	3	-2	-1	3	-2	1	-1	0
6.0	4	-2	-0	1	1	-3	3	-2	1	-0
7.0	-5	3	-1	1	-1	2	-3	4	-3	2
8.0	3	-1	1	-1	-0	0	2	-4	5	-3
9.0	-1	1	-2	1	1	-2	0	4	-5	4
10.0	-2	-0	3	-2	-0	2	-1	-2	5	-4
11.0	4	-1	-2	2	-1	0	-0	2	-3	2
12.0	-7	4	0	-1	1	-3	3	-2	2	0
13.0	8	-5	1	1	-2	5	-6	4	-0	-3
14.0	-8	6	-2	0	1	-5	7	-5	1	3
15.0	6	-5	3	-2	1	3	-7	7	-4	0
16.0	-4	4	-4	4	-3	-1	5	-8	8	-4
17.0	3	-2	2	-3	3	-0	-4	8	-9	6
18.0	-2	2	-1	1	-2	1	2	-5	6	-4
19.0	2	-3	1	-1	2	-1	-1	3	-3	2
20.0	-1	2	-1	2	-2	0	2	-3	2	1
21.0	-2	2	-2	-0	1	-4	1	4	-1	-2
22.0	6	-12	13	-7	2	-3	4	-3	0	3
23.0	-12	25	-30	18	-5	2	-2	1	2	-3
24.0	20	-30	37	-22	5	-1	1	-3	1	4
25.0	-26	23	-25	14	-2	-1	-0	-1	4	-5
26.0	28	-12	8	-5	0	1	1	-4	5	5
27.0	-20	5	-1	2	-1	0	-2	1	2	-3
28.0	8	-2	1	-2	2	-1	3	-3	2	-1
29.0	1	-1	0	1	-1	1	-3	5	-5	4
30.0	-4	3	-2	1	-1	-1	3	-4	4	-2
31.0	5	-4	3	-3	1	0	-2	3	-2	-1
32.0	-4	5	-4	3	-2	0	1	-2	1	1
33.0	4	-5	6	-4	1	0	-1	2	-2	1
34.0	-2	5	-7	5	-2	-1	2	-3	2	3
35.0	0	-3	7	-7	3	1	-4	4	2	2
36.0	-0	5	-5	6	-4	-2	3	0	4	-15
37.0	2	-2	3	-3	1	-1	0	8	-16	3
38.0	-3	1	0	-1	0	-1	9	-15	0	14
39.0	3	-1	-1	2	-2	8	-9	-6	14	-2
40.0	-2	2	-1	-3	6	0	-11	9	4	-7
41.0	0	-2	2	1	-0	-7	2	15	-12	-1
42.0	2	-0	-0	3	-5	-8	20	-10	-2	1
43.0	-2	3	-2	-1	-3	10	-5	-5	3	3
44.0	1	-5	6	-4	3	3	-6	2	2	-2
45.0	1	4	-8	5	2	-2	-1	-0	1	2
46.0	-2	-2	5	-3	-1	-0	0	3	-1	-4
47.0	2	-0	-1	1	1	-2	1	-1	-1	4
48.0	-2	1	-0	0	-2	2	0	-1	3	-4
49.0	1	-1	1	0	1	-2	1	1	-3	1
50.0	-1	1	-1	0	-1	3	-3	0	2	0
51.0	1	0	-0	0	1	-3	2	-0	-0	-0
52.0	-1	-2	3	-2	-0	1	-0	-1	0	-0
53.0	1	3	-3	2	0	0	-3	4	-2	1
54.0	-1	-2	1	0	-1	-1	5	-6	3	-0
55.0	-1	2	1	-2	1	2	-6	7	-4	-1
56.0	4	-4	1	1	-0	-2	5	-7	5	0
57.0	-6	6	-3	1	-1	1	-3	5	-5	2
58.0	4	-5	4	-3	1	-1	1	-3	4	-2
59.0	-1	1	-1	2	-2	3	-3	3	-2	1
60.0	-1	2	-2	-0	3	-5	5	-4	2	0
61.0	1	-3	3	-1	-2	4	-6	5	-2	-2
62.0	-1	4	-3	1	-0	-2	4	-4	1	3
63.0	3	-5	3	-1	1	-0	-2	2	-0	-4
64.0	-3	4	-1	-0	-1	2	-1	0	-0	3
65.0	1	0	-2	2	1	-3	3	-2	0	-1
66.0	2	-3	3	-2	-1	3	-3	1	1	0
67.0	-0	-0	-0	-0	-0	-0	-0	-0	-0	-0

UCRL-10074
Fig. 19